Journal of Electrochemical Science and Technology
Vol. 3, No. 1, 2012, 29-34
http://dx.doi.org/10.5229/JECST.2012.3.1.29

THE KOREAN ELECTROCHEMICAL SOCIETY **Journal of Electrochemical Science and Technology**

Crystal Structure Changes of $LiNi_{0.5}Co_{0.2}Mn_{0.3}O_2$ Cathode Materials During the First Charge Investigated by in situ XRD

Sangwoo Lee[a], Donghyuk Jang[a], Jeongbae Yoon[a], Yong-Hun Cho[b], Yun-Sung Lee[c], Do-Hoon Kim[d], Woo-Seong Kim[e], and Won-Sub Yoon[a,†]

[a]*Department Of Energy Science, Sungkyunkwan University, 300 Suwon-si, Gyeonggi-do 440-746, Korea*
[b]*School of Advanced Materials Engineering, Kookmin University, 861-1 Jeongneung-dong, Seongbuk-gu, Seoul 136-702, Republic of Korea*
[c]*Faculty of Applied Chemical Engineering, Chonnam National University, Gwang-ju 500-757, Korea*
[d]*Kokam, Yachon-ri Gayagok-myon Nonsan-si, Chungcheongnam-do 483-42, Korea*
[e]*Daejung EM Co.LTD, Incheon 405-820, Republic of Korea*

ABSTRACT :

The structural changes of $Li_{1-x}Ni_{0.5}Co_{0.2}Mn_{0.3}O_2$ cathode material for lithium ion battery during the first charge was investigated in comparison with $Li_{1-x}Ni_{0.8}Co_{0.15}Al_{0.05}O_2$ using a synchrotron based in situ X-ray diffraction technique. The structural changes of these two cathode materials show similar trend during first charge: an expansion along the c-axis of the unit cell with contractions along the a- and b-axis during the early stage of charge and a major contraction along the c-axis with slight expansions along the a- and b-axis near the end of charge at high voltage limit. In $Li_{1-x}Ni_{0.5}Co_{0.2}Mn_{0.3}O_2$ cathode, however, the initial unit cell volume of H2 phase is bigger than that of H1 phase since the c-axis undergo large expansion while a- and b- axis shrink slightly. The change in the unit cell volume for $Li_{1-x}Ni_{0.5}Co_{0.2}Mn_{0.3}O_2$ during charge is smaller than that of $Li_{1-x}Ni_{0.8}Co_{0.15}Al_{0.05}O_2$. This smaller change in unit cell volume may give the $Li_{1-x}Ni_{0.5}Co_{0.2}Mn_{0.3}O_2$ cathode material a better structural reversibility for a long cycling life.

Keywords : Lithium ion battery, Cathode material, $LiNi_{0.5}Co_{0.2}Mn_{0.3}O_2$, In situ X-ray diffraction

Received February 24, 2012 : Accepted March 7, 2012

1. Introduction

$LiCoO_2$ has been most widely used as positive electrode material because of its good cycleability,[1-3] acceptable discharge capacity, high rate capability, and reasonable thermal stability in common electrolytes.[4] Lithium extraction from layered $LiCoO_2$ is explained on the basis of the relative energies of the $Co^{3+/4+}$ redox couple.[5] However, there has been extensive research focused on finding new positive electrode materials with higher capacity and better cycle life to replace $LiCoO_2$ in Lithium-ion batteries. Therefore, many research groups are studying of new materials. One of the new cathode materials, $LiNi_{0.8}Co_{0.15}Al_{0.05}O_2$ has demonstrated some positive points in high power applications such as hybrid electric vehicles (HEV). Michel Broussely et al. reported the significant improvements in the safety characteristics and cycleability of $LiNi_{0.8}Co_{0.15}Al_{0.05}O_2$ over $LiNiO_2$ cathode material.[6] Recently, $LiNi_{1-y-z}Mn_yCo_zO_2$ cathode materials have attracted a lot of interest due to better electrochemical properties and safety.[7,8] Among $LiNi_{1-y-z}Mn_yCo_zO_2$ cathode materials, $LiNi_{0.5}Co_{0.2}Mn_{0.3}O_2$ is one of the optimized compositions in $LiNi_{1-y-z}Mn_yCo_zO_2$ cathode materials series, which is now commercialized in some of the major battery companies. In this study, $LiNi_{0.5}Co_{0.2}Mn_{0.3}O_2$ material was

†Corresponding author. Tel.: +82-31-299-6276
E-mail address: wsyoon@skku.edu

studied using synchrotron based X-ray diffraction. During the first charge, the electrochemical performance and properties of cathode materials for lithium-ion batteries are related with the structural changes and their crystal structure.

2. Experimental

The slurry for cathode was prepared by mixing of 92% $LiNi_{0.5}Co_{0.2}Mn_{0.3}O_2$ (Daejung EM Co. LTD), 4% carbon black (Chevron) as conductor material, 4% polyvinylidene fluoride (Kureha) binder with N Methyl pyrrolidone solvent. The cathode film was formed on the Al foil current collector by slurry coating technique. The coin cell (2032 type) was made of a Li foil for anode, a separator (Celgard), and as-prepared cathode with a 1.3 M $LiPF_6$ electrolyte in a 3:7 ethylene carbonate/diethyl carbonate solvent. The in situ XRD cells were assembled in an argon-filled glove box. The Kapton windows were used in the in situ cell for synchrotron based in situ x-ray diffraction. These in situ experiments have been described in detail elsewhere.[9] In situ XRD spectra were collected on beam line 10B XRD KIST-PAL (with λ = 0.9961 Å wavelength) at the Pohang Light Source (PLS) at Pohang Accelerator Laboratory using MAR345 image plate detector. The two theta angles of all the XRD spectra presented in this paper have been recalculated and converted to corresponding angles for λ = 1.54 Å, which is the wavelength of conventional X-ray tube source with Cu Ka radiation, for easy comparison with other published results in paper.

3. Results and Discussion

Synchrotron-based in situ XRD technique was used for studying the structural changes of $Li_{1-x}Ni_{0.5}Co_{0.2}Mn_{0.3}O_2$ during first charge. The first charge curve of $Li_{1-x}Ni_{0.5}Co_{0.2}Mn_{0.3}O_2$ is plotted in Fig. 1. The in situ cell was charged to the 5 V cut-off limit with a specific charge capacity about 279 mAh/g using a constant current condition at C/7 rate. During the first charge, 178 XRD scans were continuously collected as indicated in Fig. 1. Fig. 2 and 3 show the in situ XRD patterns of a $Li_{1-x}Ni_{0.5}Co_{0.2}Mn_{0.3}O_2$ cathode during the first charge at a C/7 rate. For easy comparison purpose, the two theta angles of all the XRD patterns presented in this paper have been recalculated and converted to the corresponding angles for a λ = 1.54 Å, which is the wavelength of a conventional X-ray tube source with Cu-Kα radiation. The missing data in scans of 138 through 145 were due to the X-ray beam being unavailable. These in situ XRD patterns are plotted in Fig. 2 for the 2θ angle regions with Bragg reflections (indexed based on a hexagonal unit cell) from (003) to (105), and in Fig. 3 for the Bragg reflections from (107) to (113). The scan numbers marked in Fig. 2 and 3 correspond to the numbers marked on the first charge curve in Fig. 1. The peaks in the XRD spectra can be indexed to a hexagonal phase similar to that indexed by Yang et al. for $LiNiO_2$.[10] Two hexagonal phases (H1 and H2) can be clearly identified and their corresponding Bragg peaks are indexed in Figs. 2 and 3. At the end of charge, the formation of the third hexagonal phase H3, indicated by a shoulder formed on the higher 2θ angle side of (003) peak of H2, can be observed.

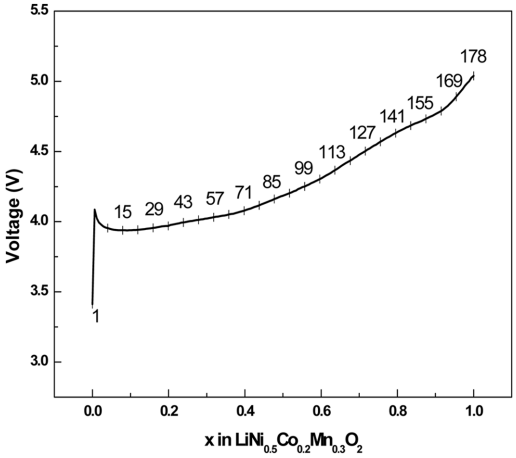

Fig. 1. The first charge curves of Li/ $LiNi_{0.5}Co_{0.2}Mn_{0.3}O_2$ cell at rate of C/7 to 5.0 V.

The c-axis in the hexagonal unit cell is normal to the set of atomic layers that contribute to the (003) and (006) reflections. Therefore, changes in the length of c-axis can be monitored by the variation of the 2θ angle positions of (003) and (006) reflections. Similarly, the (110) reflection arises from a set of atomic planes that are parallel to the c-axis. Therefore, the 2θ angle positions of (110) reflection are sensitive only to the changes in the length of a- or b-axis in the unit cell. The other indexed reflections from the cathode materials have coupled contributions from a- or b- axis and c-axis. The structural changes observed in Fig. 2 are

similar to the phase transitions reported by Yang et al.[10] for $LiNiO_2$ during the first charge. In that study, Yang et al. observed a set of new peaks, which was indexed to a new hexagonal phase H2, emerges at the expense of the original hexagonal phase H1 during first charge (between 3.9 and 4.2 V). The (003) peak of the newly formed phase occurs at a lower 2θ angle than the original phase, indicating that the newly formed phase has a larger c-axis, while the (101) and (110) peaks of the new H2 phase emerge at higher 2θ angles than those for H1, indicating a shorter length in a and b axis. It can be seen in Fig. 2, during scan 8-22 in first charge for $Li_{1-x}Ni_{0.5}Co_{0.2}Mn_{0.3}O_2$ cathode, a (003)H2 peak representing the H2 phase emerges at the lower 2θ angle side of (003)H1, while the (101)H2 emerges at the higher 2θ angle side of (101)H1. This is almost the same as what had been reported for the $LiNiO_2$ cathode.[10] During the phase transition from H1 to H2 (scan 8-50), with the decreasing intensities of the Bragg peaks representing H1 phase, the 2θ angle positions for both (003)H1 and (101)H1 remain the same. During the same charge period, with the increasing intensities of the Bragg peaks representing H2 phase, the (003)H2 position shifts continuously to lower angles while (101)H2 position keep moving to higher angles. This indicates that the c-axis of the H2 phase expands while the a-b plane contacts during early stage of charge. When charged to high voltage during scan 106-178, the position of (003)H2 peak changes moving direction towards the higher angles and the peak width broadens significantly. At the end of charge at 5 V, a new peak emerged at the right shoulder of (003)H2 peak, indicating the formation of the H3 phase with even shorter c-axis. However, in comparison with the structural changes of $LiNiO_2$ reported by Yang et al.,[10] for $Li_{1-x}Ni_{0.5}Co_{0.2}Mn_{0.3}O_2$ cathode, the length of c-axis of H3 unit cell is larger, and the phase transition from H2 to H3 was incomplete. From scan 57 to scan 178, the position change of (101) peak is hardly noticeable. The position of (101) peak mainly represents the changes of a-axis, but also has a minor contribution (1/3 in weight) from the c-axis.[10] Therefore, in order to get precise information about the changes in a-b plane, the position changes of (110)H2, which has pure a-b contribution with no c-axis contribution, need to be examined.

Using the (220)Al reflection (from the Al current collector in the in situ cell) as internal standard, the position changes of (110)H2 can be clearly identified in Fig. 3. As shown in Fig. 3, during scan 1-99 (110)H2 follows the similar trend as (101)H2 in Fig. 2: emerges at the higher angle side of (110)H1 starting at

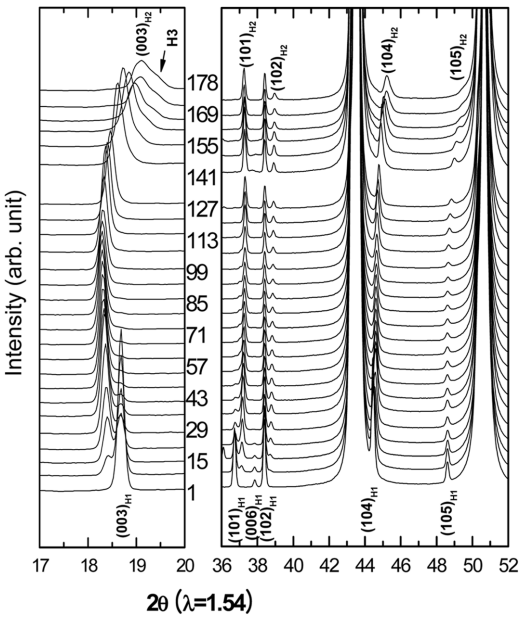

Fig. 2. The in situ XRD patterns of $Li/LiNi_{0.5}Co_{0.2}Mn_{0.3}O_2$ from the (003) to (105) region during the first charge at rate of C/7.

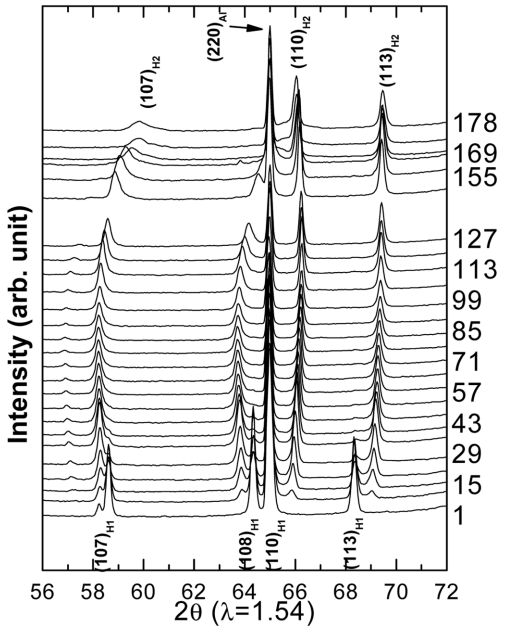

Fig. 3. The in situ XRD patterns of $Li/LiNi_{0.5}Co_{0.2}Mn_{0.3}O_2$ from the (107) to (113) region during the first charge at rate of C/7.

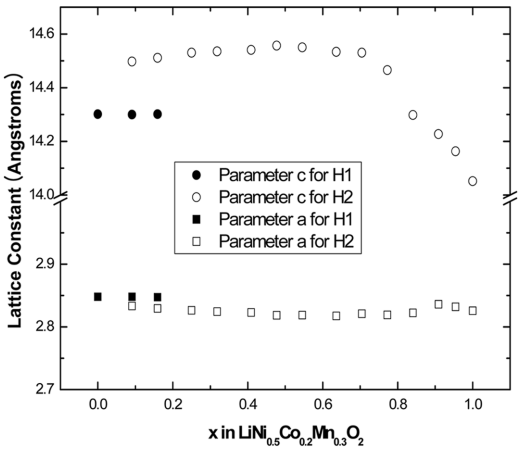

Fig. 4. The lattice parameters of $Li/LiNi_{0.5}Co_{0.2}Mn_{0.3}O_2$ during the first charge. The hexagonal phase H1 lattice parameters are marked as filled circles and squares, and the new hexagonal phase H2 as emptied figures.

scan 8, and then moves to higher angles from scan 8-99. However, from scan 127-178, the (110) peak shows a tendency in shifting to smaller angles, reassemble the structural change feature of $LiCoO_2$ at high voltage charging reported by Yang et al.[9] These observations suggest that during scan 127-178, the a- and b-axis of the unit cell expand a small amount, when the c-axis having a major contraction. The position changes of (10l) peaks in Figs. 2 and 3 can be explained in the following way. The position changes of (10l) reflections with larger l values, such as (108), follow the trends seen for the (003) peaks, while those with smaller l values, such as (101), follow the (110) peak. As the values of l increases, the influence to the peak position by the c-axis increase. Therefore, the shift in the (108) reflection is similar to the changes in the (003) reflection while the shift in the (101) reflection basically follows the (110) reflection. Finally, the peak intensity of the (006) reflection becomes very weak after scan 29 and cannot be recognized.

The lattice parameters obtained from least-squares refinements using the in situ XRD data are shown as a function of x in $Li_{1-x}Ni_{0.5}Co_{0.2}Mn_{0.3}O_2$ in Fig. 4. $Li_{1-x}Ni_{0.5}Co_{0.2}Mn_{0.3}O_2$ underwent a structural phase transition from a hexagonal phase H1 to a new hexagonal phase H2 starting from the early stage of charge (scan 8). The H1 phase co-existed with H2 phase until scan 29. In this two-phase co-existence region, the lattice parameters for H1 phase (a = 2.848 Å and c = 14.301 Å) remain the same while the lattice parameters for H2 phase change significantly. The lattice parameters of H2 phase show an initial expansion along the c-axis and a simultaneous contraction along

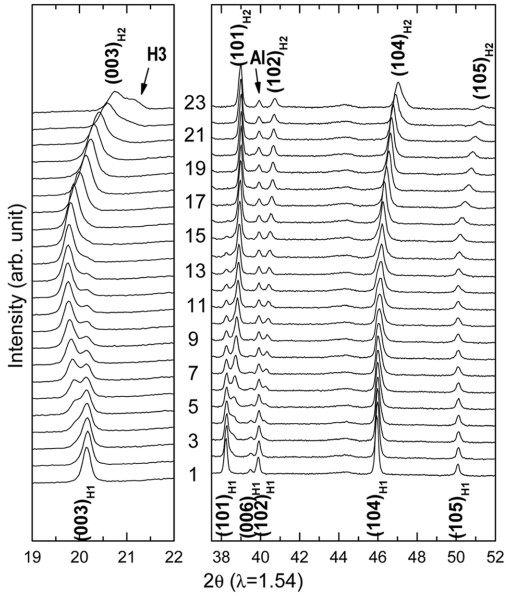

Fig. 5. The in situ XRD patterns of $Li/LiNi_{0.8}Co_{0.15}Al_{0.05}O_2$ from the (003) to (105) region during the first charge at rate of C/5.

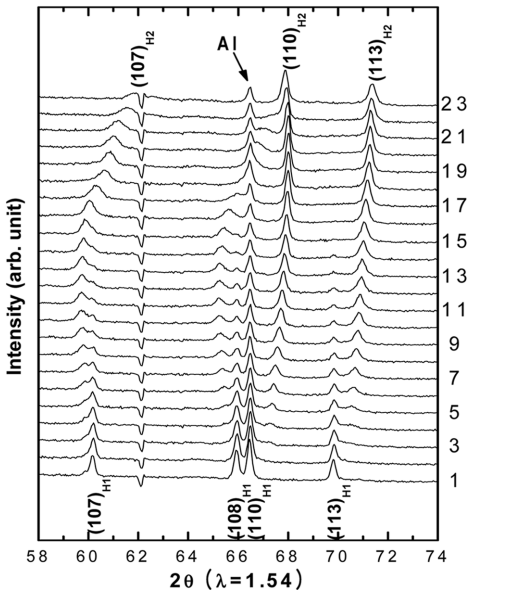

Fig. 6. The in situ XRD patterns of $Li/LiNi_{0.8}Co_{0.15}Al_{0.05}O_2$ from the (107) to (113) region during the first charge at rate of C/5.

the a- and b-axis during early stage of charge. Towards the end of charge there is a major contraction along the c-axis and a slight expansion along the a- and b-axis. The formation of the third hexagonal phase H3 with a c-axis shorter than H2 is observed. For $0 \le x \le 1.0$ in $Li_{1-x}Ni_{0.5}Co_{0.2}Mn_{0.3}O_2$, the c-axis elongated from 14.207 Å to 14.534 Å and then shrank back to 14.052 Å while the a-axis gradually shortened from 2.848 Å to 2.826 Å. Consequently, the unit cell volume decreased from 100.457 Å^3 to 97.164 Å^3. The unit cell volume decreases by ~3.3% during the first charge from x = 0.0 to x = 1.0 in $Li_{1-x}Ni_{0.5}Co_{0.2}Mn_{0.3}O_2$ compared to that of pristine $LiNi_{0.5}Co_{0.2}Mn_{0.3}O_2$.

The comprehensive structural changes of $LiNi_{0.5}Co_{0.2}Mn_{0.3}O_2$ cathode material during charge are different from those of previously reported nickel-based layered materials even though all the nickel-based layered materials show some general trends in structural properties. Therefore, it would be interesting to compare the detailed structural changes of $LiNi_{0.5}Co_{0.2}Mn_{0.3}O_2$ with $LiNi_{0.8}Co_{0.15}Al_{0.05}O_2$ system, which is one of the well-reported nickel layered materials. In order to compare the structural behaviors of the $LiNi_{0.5}Co_{0.2}Mn_{0.3}O_2$ and the $LiNi_{0.8}Co_{0.15}Al_{0.05}O_2$ system in more detail, the published data for Fig. 2 and 3 of [11] for $LiNi_{0.8}Co_{0.15}Al_{0.05}O_2$ were re-processed in similar format as used in this study and are plotted in Fig. 5 and 6 (23 XRD patterns are collected during first charge with 5.2 V cut-off voltage; the charging curve and more detailed information have been reported in [11]). In both systems, the similarity is that the new H2 phases in both materials show a shorter "a" and a longer "c" axis in the early charge. Then, the original H1 phase of both layered materials does not show any change in lattice parameters. However, in the $LiNi_{0.5}Co_{0.2}Mn_{0.3}O_2$ system, the changes in lattice parameters from H1 (a = 2.848 Å and c = 14.301 Å from scan 8 in Fig. 2) to H2 (a = 2.826 Å and c = 14.502 Å from scan 8 in Fig. 2) are clearly smaller than those in the $LiNi_{0.8}Co_{0.15}Al_{0.05}O_2$ system (a = 2.866 Å and c = 14.207 Å for H1, a = 2.815 Å and c = 13.856 Å for H2, from scan 9 in Fig. 5 and 6). This reflected in the XRD patterns in Fig. 2, where the peak separation of H1 and H2 (101) reflection was severely reduced, while the peak separation of H1 and H2 (003)reflection was hardly observed. The other differences between the two layered materials are the following: The original H1 phase of $Li_{1-x}Ni_{0.5}Co_{0.2}Mn_{0.3}O_2$ disappears in the early state of charge (at scan 50 of the 178 total scans). However, the original H1 phase of $Li_{1-x}Ni_{0.8}Co_{0.15}Al_{0.05}O_2$ is observable well passed the middle point of charge curve (up to scan 15 out of 23 scans).

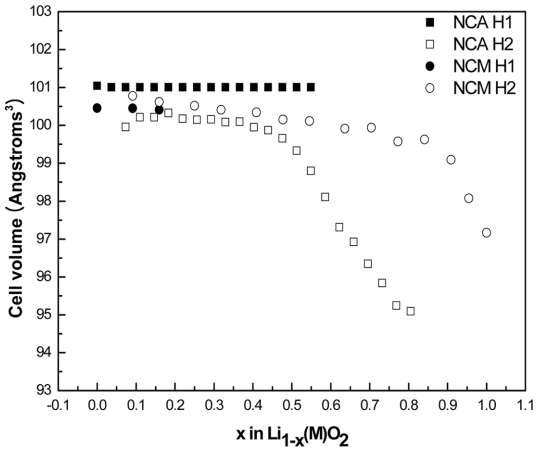

Fig. 7. The unit cell volume of Li/$LiNi_{0.5}Co_{0.2}Mn_{0.3}O_2$ during the first charge. The $LiNi_{0.8}Co_{0.15}Al_{0.05}O_2$ unit cell volume is marked as filled figures, and the $LiNi_{0.5}Co_{0.2}Mn_{0.3}O_2$ unit cell volume with emptied figures.

Fig. 7 shows changes in the unit cell volumes of $Li_{1-x}Ni_{0.5}Co_{0.2}Mn_{0.3}O_2$ and $Li_{1-x}Ni_{0.8}Co_{0.15}Al_{0.05}O_2$ as a function of x during first charge. For $0 \le x \le 0.8$ in $Li_{1-x}Ni_{0.8}Co_{0.15}Al_{0.05}O_2$, the c-axis elongated from 14.207 Å to 14.562 Å and then shrank back to 13.856 Å while the a-axis gradually shortened from 2.866 Å to 2.815 Å. Consequently, the unit cell volume decreased from 101.05 Å^3 to 95.09 Å^3. The unit cell volume decreases by ~5.9% during first charge from x = 0.0 to x = 0.8 in $Li_{1-x}Ni_{0.8}Co_{0.15}Al_{0.05}O_2$ compared to that of pristine $Li_{1-x}Ni_{0.8}Co_{0.15}Al_{0.05}O_2$. For $0 \le x \le 1.0$ in $Li_{1-x}Ni_{0.5}Mn_{0.3}Co_{0.2}O_2$, the c-axis elongated from 14.301 Å to 14.502 Å and then shrank back to 14.052 Å while the a-axis gradually shortened from 2.848 Å to 2.826 Å leading to the decrease in the unit cell volume from 100.46 Å^3 to 97.16 Å^3. Comparing the lattice parameters in both layered materials during charge, the unit cell change for $Li_{1-x}Ni_{0.5}Mn_{0.3}Co_{0.2}O_2$ (~3.28% for x = 0.0–1.0) is smaller than that for $Li_{1-x}Ni_{0.8}Co_{0.15}Al_{0.05}O_2$ (~5.9% for x = 0.0–0.8). This relatively smaller change in unit cell volume may give the $Li_{1-x}Ni_{0.5}Mn_{0.3}Co_{0.2}O_2$ material a better structural reversibility for a longer cycling life.

4. Conclusions

The structural changes of $Li_{1-x}Ni_{0.5}Co_{0.2}Mn_{0.3}O_2$ cathode material during first charge have been studied in comparison with previously reported $Li_{1-x}Ni_{0.8}Co_{0.15}Al_{0.05}O_2$ cathode. The lattice parameters changes of both cathodes, $Li_{1-x}Ni_{0.5}Co_{0.2}Mn_{0.3}O_2$ and $Li_{1-x}Ni_{0.8}Co_{0.15}Al_{0.05}O_2$, show similar trend during first charge. In the early charge state, there was an initial expansion along the c-axis and contraction along the a- and b- axis simultaneously in the unit cells. Towards to the end of charge, the c-axis shows a major contraction while the a- and b- axes show a small expansion. In $Li_{1-x}Ni_{0.5}Co_{0.2}Mn_{0.3}O_2$ cathode, however, the initial unit cell volume of H2 phase is bigger than that of H1 phase since the c-axis undergo large expansion while a- and b- axes shrink slightly. After phase transition from H1 to H2, it retain the similar unit cell volume for a while (Until $x = 0.7$). For $0.7 \leq x$ in $Li_{1-x}Ni_{0.5}Co_{0.2}Mn_{0.3}O_2$, the c-axis starts shrink back. However, the c-axis of $Li_{1-x}Ni_{0.5}Co_{0.2}Mn_{0.3}O_2$ ($0.7 \leq x$) shrink slower than $Li_{1-x}Ni_{0.8}Co_{0.15}Al_{0.05}O_2$ ($0.45 \leq x$), a better structural stability of $Li_{1-x}Ni_{0.5}Co_{0.2}Mn_{0.3}O_2$ can be anticipated. At the end of charge, moreover, the change in the unit cell volume for $Li_{1-x}Ni_{0.5}Co_{0.2}Mn_{0.3}O_2$ is smaller than that of $Li_{1-x}Ni_{0.8}Co_{0.15}Al_{0.05}O_2$. This smaller change in unit cell volume may lead to a better structural reversibility for a long cycling life.

Acknowledgements

This work at Sungkyunkwan University was supported by Honam Leading Industry Office (20096403) of Ministry of Knowledge Economy and WCU (World Class University) program through the National Research Foundation of Korea by the Ministry of Education, Science and Technology (R31-2008-10029).

References

1. K. Mizushima, P.C. Jones, P.C. Wiseman and J.B. Goodenough, *Mater. Res. Bull*., **15**, 783 (1980).
2. T. Nagaura and K. Tozawa, *Prog. Batt. Solar Cells*, **9**, 209 (1991).
3. K. Ozawa, *Solid State Ionics*, **69,** 212 (1994).
4. D.D. MacNeil and J.R. Dahn, *J. Electrochem. Soc.*, **149**, A912 (2002).
5. R. Gupta and A.J. Manthiram, *Solid State Chem.*, **121**, 483 (1996**)**.
6. M. Broussely, Abstract No. 415, eleventh international meeting on lithium batteries, Monterey, California, USA, 23-28 (2002).
7. T. Ohzuku and Y. Makimura, *Chem. Lett.*, 642 (2001).
8. Z. Lu, D.D. MacNeil and J.R. Dahn, *Electrochem. Solid State Lett.*, **4**, A200 (2001).
9. M. Balasubramanian, X. Sun, X.Q. Yang and J. McBreen, *J. Power Sources*, **92**, 1 (2001).
10. M.S. Whittingham, *Chem. Rev.*, **104**, 4271 (2004).
11. X.Q. Yang, X. Sun, and J. McBreen, *Electrochem. Commun.*, **8**, 1257 (2006).